

MLMC: Machine Learning Monte Carlo for Lattice Gauge Theory

Sam Foreman,^{a,*} Xiao-Yong Jin^{a,b} and James C. Osborn^{a,b}

^a*Leadership Computing Facility, Argonne National Laboratory,
9700 S. Cass Ave, Lemont IL, USA*

^b*Computational Science Division, Argonne National Laboratory,
9700 S. Cass Ave, Lemont IL, USA*

E-mail: foremans@anl.gov, xjin@anl.gov, osborn@alcf.anl.gov

We present a trainable framework for efficiently generating gauge configurations, and discuss ongoing work in this direction. In particular, we consider the problem of sampling configurations from a 4D $SU(3)$ lattice gauge theory, and consider a generalized leapfrog integrator in the molecular dynamics update that can be trained to improve sampling efficiency. Code is available online at [12hmc-qcd](https://github.com/12hmc-qcd).

*The 40th International Symposium on Lattice Field Theory (Lattice 2023)
July 31st - August 4th, 2023
Fermi National Accelerator Laboratory*

*Speaker

1. Introduction

We would like to calculate observables O :

$$\langle O \rangle \propto \int [\mathcal{D}x] O(x) \pi(x) \quad (1)$$

where $\pi(x) \propto e^{-\beta S(x)}$ is our target distribution. If these were independent, we could approximate the integral as $\langle O \rangle \simeq \frac{1}{N} \sum_{n=1}^N O(x_n)$ with variance

$$\sigma_O^2 = \frac{1}{N} \text{Var} [O(x)] \implies \sigma_O \propto \frac{1}{\sqrt{N}}. \quad (2)$$

Instead, nearby configurations are correlated, causing us to incur a factor of τ_{int}^O in the variance expression

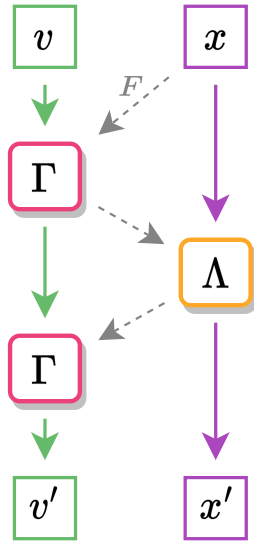
$$\sigma_O^2 = \frac{\tau_{\text{int}}^O}{N} \text{Var} [O(x)]. \quad (3)$$

1.1 Hamiltonian Monte Carlo (HMC)

The typical approach [8, 9] is to use Hamiltonian Monte Carlo (HMC) algorithm for generating configurations distributed according to our target distribution $\pi(x)$. This can be done by sequentially constructing a chain of states $\{x_0, x_1, x_2, \dots, x_i, \dots, x_n\}$, such that, as $n \rightarrow \infty$:

$$\{x_i, x_{i+1}, x_{i+2}, \dots, x_n\} \sim \pi(x). \quad (4)$$

Figure 1: Leapfrog update.



To do this, we begin by introducing a fictitious momentum¹ $v \sim \mathcal{N}(0, 1)$ normally distributed, independent of x . We can write the joint distribution $\pi(x, v)$ as

$$\pi(x, v) = \pi(x)\pi(v) \propto e^{-S(x)} e^{-\frac{1}{2}v^T v} \quad (5)$$

$$= e^{-[S(x) + \frac{1}{2}v^T v]} \quad (6)$$

We can evolve the Hamiltonian dynamics of the $(\dot{x}, \dot{v}) = (\partial_v H, -\partial_x H)$ system using operators $\Gamma : v \rightarrow v'$ and $\Lambda : x \rightarrow x'$. Explicitly, for a single update step of the leapfrog integrator:

$$\tilde{v} := \Gamma(x, v) = v - \frac{\varepsilon}{2} F(x) \quad (7)$$

$$x' := \Lambda(x, \tilde{v}) = x + \varepsilon \tilde{v} \quad (8)$$

$$v' := \Lambda(x', \tilde{v}) = \tilde{v} - \frac{\varepsilon}{2} F(x'), \quad (9)$$

where we've written the force term as $F(x) = \partial_x S(x)$. Typically, we build a trajectory of N_{LF} leapfrog steps $(x_0, v_0) \rightarrow (x_1, v_1) \rightarrow \dots \rightarrow (x', v')$, and propose x' as the next state in our chain. This proposal state is then accepted according to the Metropolis-Hastings criteria [25]

$$A(x'|x) = \min \left\{ 1, \frac{\pi(x')}{\pi(x)} \left| \frac{\partial x'}{\partial x} \right| \right\}. \quad (10)$$

¹Here \sim means *is distributed according to*.

2. Method

Unfortunately, HMC is known to suffer from long auto-correlations and often struggles with multi-modal target densities. To combat this, we propose building on the approach from [8–10]. We introduce two (invertible) neural networks $\mathbf{xNet} : (x, v) \rightarrow (\alpha_x, \beta_x, \gamma_x)$, $\mathbf{vNet} : (x, F) \rightarrow (\alpha_v, \beta_v, \gamma_v)$. Here, (α, β, γ) are all of the same dimensionality as x and v , and are parameterized by a set of weights θ . These network outputs (α, β, γ) are then used in a generalized MD update (as shown in Fig 2) via:

$$\boxed{\Gamma_\theta^\pm} : (x, v) \rightarrow (x, v'), \quad (11)$$

$$\boxed{\Lambda_\theta^\pm} : (x, v) \rightarrow (x', v). \quad (12)$$

where the superscript \pm on $\Gamma_\theta^\pm, \Lambda_\theta^\pm$ correspond to the direction $d \sim \mathcal{U}(-1, +1)$ of the update.

To ensure that our proposed update remains reversible, we split the x update into two sub-updates on complementary subsets ($x = x_A \cup x_B$):

$$v' = \Gamma_\theta^\pm(x, v) \quad (13)$$

$$x' = x_B + \Lambda_\theta^\pm(x_A, v') \quad (14)$$

$$x'' = x'_A + \Lambda_\theta^\pm(x'_B, v') \quad (15)$$

$$v'' = \Gamma_\theta^\pm(x'', v') \quad (16)$$

2.1 Algorithm

1. input: x

- Re-sample $v \sim \mathcal{N}(0, 1)$
- Construct initial state $\xi := (x, v)$

2. forward: Generate proposal ξ' by passing initial ξ through N_{LF} leapfrog layers:

$$\xi \xrightarrow{\text{LF Layer}} \xi_1 \rightarrow \dots \rightarrow \xi_{N_{\text{LF}}} = \xi' := (x'', v'') \quad (17)$$

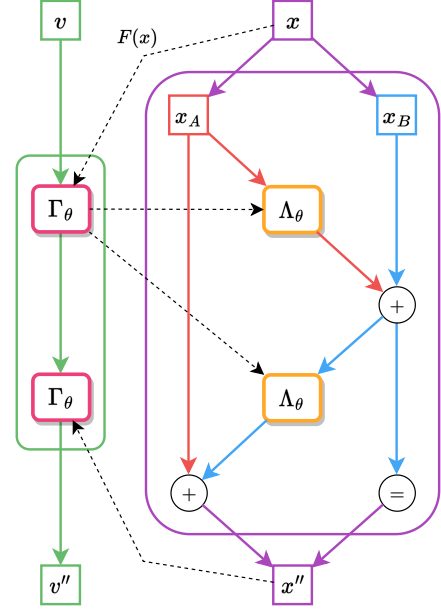
- Metropolis-Hastings accept / reject:

$$A(\xi'|\xi) = \min \left\{ 1, \frac{\pi(\xi')}{\pi(\xi)} |\mathcal{J}(\xi', \xi)| \right\}, \quad (18)$$

where $|\mathcal{J}(\xi', \xi)|$ is the determinant of the Jacobian.

3. backward: (if training)

Figure 2: Generalized MD update.



- Evaluate the loss function $\mathcal{L}(\xi', \xi)$ and back propagate

4. **return:** x_{i+1}

- Evaluate MH criteria (Eq. 18) and return accepted config:

$$x_{i+1} \leftarrow \begin{cases} x'' & \text{w/ prob. } A(\xi'|\xi) \\ x & \text{w/ prob. } 1 - A(\xi'|\xi) \end{cases} \quad (19)$$

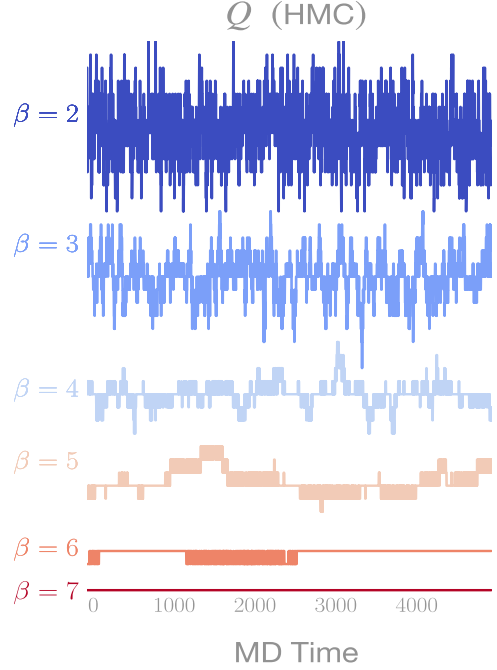
3. Lattice Gauge Theories

3.1 2D $U(1)$ Model

We build upon the approach originally introduced in [17], which was successfully applied to the 2D $U(1)$ lattice gauge model in [8–10]. In particular, we are interested in measuring the (scalar) topological charge $Q \in \mathbb{Z}$ on the lattice. Since different lattice configurations with the same value of Q are related by a gauge transformation, they do not meaningfully contribute to our statistics.

Because of this, we would like to generate configurations from different *topological sectors* (characterized by different values of Q) to reduce uncertainty in our statistical estimates. By repeating this procedure at increasing spatial resolution² ($\beta \propto 1/a$), we are able to extrapolate our estimates to the continuum limit where they can be compared with experimental measurements. Current approaches such as HMC are known to suffer from auto-correlation times which scale exponentially in this limit, significantly limiting their effectiveness. This phenomenon can be seen in Fig 3, where fluctuations in the topological charge between sequential configurations (the *tunneling rate*) $\delta Q = |Q^{i+1} - Q^i|$ decreases as $\beta = 2 \rightarrow 3 \rightarrow \dots$, and disappear completely ($Q = \text{const.}$) by $\beta = 7$.

Figure 3: $\delta Q \rightarrow 0$ with increasing β for the 2D $U(1)$ model. Image from [9].



3.1.1 Results

Results for the 2D $U(1)$ model trained at $\beta = 4$ in ≈ 25 minutes on a single NVIDIA A100 GPU, using [l2hmc-qcd](#). We provide the full [Jupyter notebook](#) containing the results in Fig 4.

3.2 4D $SU(3)$ Model

We would like to generalize this approach to handle 4D $SU(3)$ link variables $U_\mu(n) \in SU(3)$:

$$U_\mu(n) = \exp [i\omega_\mu^k(n)\lambda^k] \quad (20)$$

²Here a is the lattice spacing.

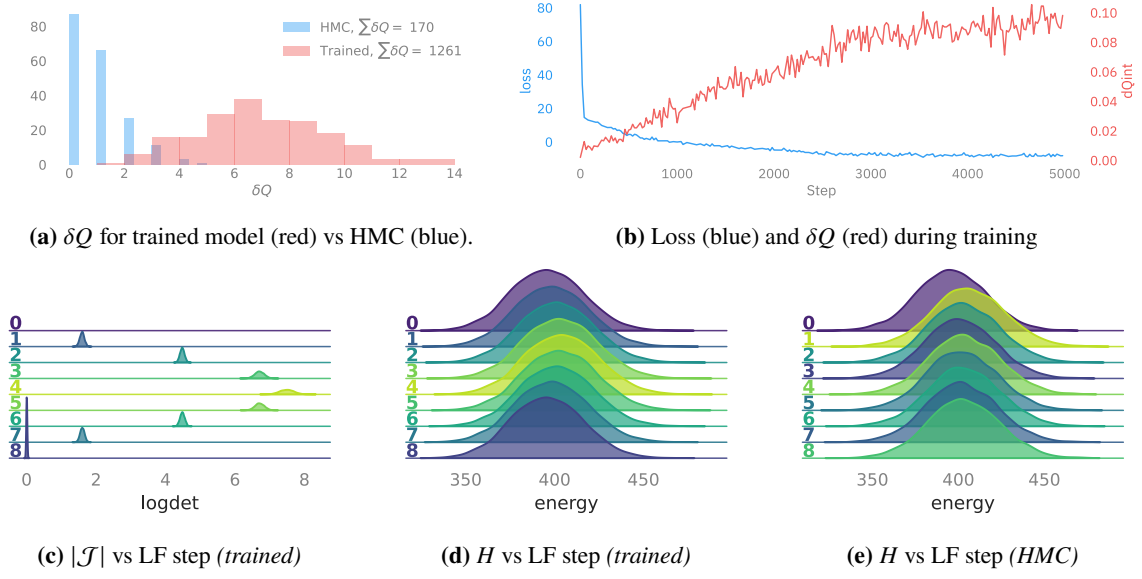


Figure 4: Results from trained 2D $U(1)$ model at $\beta = 4$. In 4d we see the energy H increasing towards the middle of the trajectory, resulting in improved tunneling rate (larger δQ) in 4a. [Jupyter notebook](#).

where $\omega_\mu^k(n) \in \mathbb{R}$ and λ^k are the generators of $SU(3)$. We consider the standard Wilson gauge action

$$S_G = -\frac{\beta}{6} \sum \text{Tr} [U_{\mu\nu}(n) + U_{\mu\nu}^\dagger(n)], \quad \text{where} \quad (21)$$

$$U_{\mu\nu}(n) = U_\mu(n)U_\nu(n + \hat{\mu})U_\mu^\dagger(n + \hat{\nu})U_\nu^\dagger(n). \quad (22)$$

3.2.1 Generic MD Updates

As before, we introduce momenta $P_\mu(n) = P_\mu^k(n)\lambda^k$ conjugate to the real fields $\omega_\mu^k(n)$. We can write the Hamiltonian as

$$H[P, U] = \frac{1}{2}P^2 + S_G[U] \implies \boxed{\frac{d\omega^k}{dt} = \frac{\partial H}{\partial P^k}}, \quad \boxed{\frac{dP^k}{dt} = -\frac{\partial H}{\partial \omega^k}}. \quad (23)$$

To update the gauge field $U_\mu = e^{i\omega_\mu^k \lambda^k}$, write $\boxed{\frac{d\omega^k}{dt} \lambda^k = P^k \lambda^k}$ and discretize with step size ε :

$$-i \log U(\varepsilon) = -i \log U(0) + \varepsilon P(0) \quad (24)$$

$$U(\varepsilon) = e^{i\varepsilon P(0)} U(0) \implies \quad (25)$$

$$\boxed{\Lambda : U \rightarrow U'} = e^{i\varepsilon P} U. \quad (26)$$

Similarly for the momentum update $\boxed{\frac{dP^k}{dt} = -\frac{\partial H}{\partial \omega^k}}$,

$$P(\varepsilon) = P(0) - \varepsilon F[U] \quad (27)$$

$$\boxed{\Gamma : P \rightarrow P'} = P - \frac{\varepsilon}{2} F[U] \quad (28)$$

where $F[U]$ is the force term (see A.1).

3.2.2 Generalized MD Update

As in Sec.2, we introduce pNet: $(U, F) \rightarrow (\alpha_P, \beta_P, \gamma_P)$ and uNet: $(U, P) \rightarrow (\cdot, \beta_U, \gamma_U)$. Note that we have omitted the U scaling term (α_U) term in this update since $U \in SU(3)$. In terms of the generalized update operators,

$$\boxed{\Gamma_\theta^\pm} : (U, P) \xrightarrow{(\alpha_P, \beta_P, \gamma_P)} (U, P') \quad (29)$$

$$\boxed{\Lambda_\theta^\pm} : (U, P) \xrightarrow{(\cdot, \beta_U, \gamma_U)} (U', P) \quad (30)$$

we can write the complete update:

$$P' = \Gamma_\theta^\pm(U, P) \quad (31)$$

$$U' = U_B + \Lambda_\theta^\pm(U_A, P') \quad (32)$$

$$U'' = U'_A + \Lambda_\theta^\pm(U'_B, P') \quad (33)$$

$$P'' = \Gamma_\theta^\pm(U'', P') \quad (34)$$

Momentum Update

In this case, our pNet : $(U, F) = (\alpha_P, \beta_P, \gamma_P)$. We can write the generalized momentum update as $P^\pm := \Gamma_\theta^\pm(U, P)$, where³:

1. forward, (+):

$$P^+ := \Gamma_\theta^+(U, P) = P \cdot e^{\frac{\varepsilon}{2} \alpha_P} - \frac{\varepsilon}{2} [F \cdot e^{\varepsilon \beta_P} + \gamma_P] \quad (35)$$

2. backward, (-):

$$P^- := \Gamma_\theta^-(U, P) = e^{-\frac{\varepsilon}{2} \alpha_P} \cdot \left\{ P + \frac{\varepsilon}{2} [F \cdot e^{\varepsilon \beta_P} + \gamma_P] \right\}. \quad (36)$$

By introducing the above modifications, we incur a factor of $\log \left| \frac{\partial P^\pm}{\partial P} \right| = \pm \frac{\varepsilon}{2} \sum \alpha_P$ in the Metropolis Hastings accept / reject $A(U'|U)$, and the sum is taken over the full trajectory.

Link Update

Similarly to the momentum update, the outputs from our uNet : $(U, P) \rightarrow (\cdot, \beta_U, \gamma_U)$ are used in the generalized link update $U^\pm := \Lambda_\theta^\pm(U, P) = e^{i\varepsilon \tilde{P}^\pm} U$ (where $\tilde{P}^\pm \in \mathfrak{su}(3)$). Explicitly:

1. forward, (+):

$$U^+ := \Lambda_\theta^+(U, P) = e^{i\varepsilon \tilde{P}^+} U, \quad \text{with} \quad \tilde{P}^+ = [P \cdot e^{\varepsilon \beta_U} + \gamma_U] \quad (37)$$

2. backward, (-):

$$U^- := \Lambda_\theta^-(U, P) = e^{i\varepsilon \tilde{P}^-} U, \quad \text{with} \quad \tilde{P}^- = e^{-\varepsilon \beta_U} \cdot [P - \gamma_U] \quad (38)$$

³Note that $(\Gamma^+)^{-1} = \Gamma^-$, i.e. $\Gamma^+ [\Gamma^-(U, F)] = \Gamma^- [\Gamma^+(U, F)] = (U, F)$, and similarly for Λ^\pm

3.3 Training

We construct a loss function using the expected squared charge difference

$$\mathcal{L}_\theta(U, U') = \mathbb{E} \left[A(U'|U) \cdot \delta_Q^2(U, U') \right], \quad (39)$$

where $\delta_Q^2(U, U') = |Q' - Q|^2$ is the squared topological charge (see A.2) difference between the initial and proposal configurations.

3.4 Results

For the trained 2D $U(1)$ model (Fig 4), we see in Fig 4c that $|\mathcal{J}|$ increases towards the middle of the trajectory, allowing for the sampler to overcome the large energy barriers between different topological sectors. This results in a greater *tunneling rate* (δQ) when compared to generic HMC. Identical behavior is observed after a short training run for the 4D $SU(3)$ model, as shown in Fig 5.

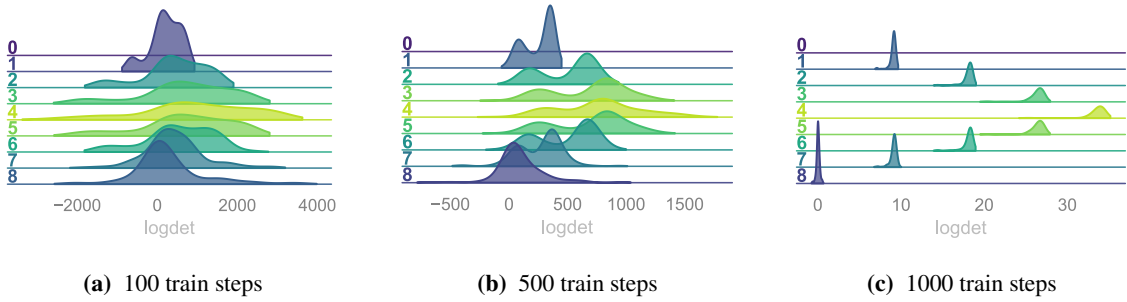


Figure 5: Evolution of $|\mathcal{J}|$ during the first 1000 training iterations for the 4D $SU(3)$ model.

4. Conclusion

In this work we've introduced a generalized MD update for generating 4D $SU(3)$ gauge configurations that can be trained to improve sampling efficiency. Note that this is a relatively simple proof of concept demonstrating how to construct such a sampler. In a future work we plan to further investigate (and quantify) the cost / benefit when compared to alternative approaches such as traditional HMC and purely generative (OT / KL-Divergence [2–4, 15]) based approaches.

5. Acknowledgements

This research used resources of the Argonne Leadership Computing Facility, which is a DOE Office of Science User Facility supported under Contract DE-AC02-06CH11357. This research was supported by the Exascale Computing Project (17-SC-20-SC), a collaborative effort of the U.S. Department of Energy Office of Science and the National Nuclear Security Administration.

References

- [1] M. Abadi, A. Agarwal, P. Barham, E. Brevdo, Z. Chen, C. Citro, G. S. Corrado, A. Davis, J. Dean, M. Devin, S. Ghemawat, I. Goodfellow, A. Harp, G. Irving, M. Isard, Y. Jia, R. Jozefowicz, L. Kaiser, M. Kudlur, J. Levenberg, D. Mane, R. Monga, S. Moore, D. Murray, C. Olah, M. Schuster, J. Shlens, B. Steiner, I. Sutskever, K. Talwar, P. Tucker, V. Vanhoucke, V. Vasudevan, F. Viegas, O. Vinyals, P. Warden, M. Wattenberg, M. Wicke, Y. Yu, and X. Zheng. TensorFlow: Large-scale machine learning on heterogeneous distributed systems. URL <http://arxiv.org/abs/1603.04467>.
- [2] M. Albergo, G. Kanwar, and P. Shanahan. Flow-based generative models for markov chain monte carlo in lattice field theory. 100(3):034515, . ISSN 2470-0010, 2470-0029. doi: 10.1103/PhysRevD.100.034515. URL <https://link.aps.org/doi/10.1103/PhysRevD.100.034515>.
- [3] M. S. Albergo, D. Boyda, D. C. Hackett, G. Kanwar, K. Cranmer, S. Racanière, D. J. Rezende, and P. E. Shanahan. Introduction to normalizing flows for lattice field theory, . URL <http://arxiv.org/abs/2101.08176>.
- [4] D. Boyda, G. Kanwar, S. Racanière, D. J. Rezende, M. S. Albergo, K. Cranmer, D. C. Hackett, and P. E. Shanahan. Sampling using $SU(n)$ gauge equivariant flows. 103(7):074504. ISSN 2470-0010, 2470-0029. doi: 10.1103/PhysRevD.103.074504. URL <http://arxiv.org/abs/2008.05456>.
- [5] G. Cossu, P. Boyle, N. Christ, C. Jung, A. Jüttner, and F. Sanfilippo. Testing algorithms for critical slowing down. 175:02008. ISSN 2100-014X. doi: 10.1051/epjconf/201817502008. URL <http://arxiv.org/abs/1710.07036>.
- [6] L. Dinh, J. Sohl-Dickstein, and S. Bengio. Density estimation using real NVP. URL <http://arxiv.org/abs/1605.08803>.
- [7] M. Favoni, A. Ipp, D. I. Müller, and D. Schuh. Lattice gauge equivariant convolutional neural networks. 128(3):032003. ISSN 0031-9007, 1079-7114. doi: 10.1103/PhysRevLett.128.032003. URL <http://arxiv.org/abs/2012.12901>.
- [8] S. Foreman, X.-Y. Jin, and J. C. Osborn. Deep learning hamiltonian monte carlo, . URL <http://arxiv.org/abs/2105.03418>.
- [9] S. Foreman, X.-Y. Jin, and J. C. Osborn. LeapfrogLayers: A trainable framework for effective topological sampling, . URL <http://arxiv.org/abs/2112.01582>.
- [10] S. A. Foreman. Learning better physics: a machine learning approach to lattice gauge theory. URL <https://iro.uiowa.edu/esploro/outputs/doctoral/9983776792002771>.
- [11] A. Gelman and C. Pasarica. Adaptively scaling the metropolis algorithm using expected squared jumped distance. ISSN 1556-5068. doi: 10.2139/ssrn.1010403. URL <http://www.ssrn.com/abstract=1010403>.

- [12] W. K. Hastings. Monte carlo sampling methods using markov chains and their applications. 57(1):97–109. ISSN 1464-3510, 0006-3444. doi: 10.1093/biomet/57.1.97. URL <https://academic.oup.com/biomet/article/57/1/97/284580>.
- [13] M. Hoffman, P. Sountsov, J. V. Dillon, I. Langmore, D. Tran, and S. Vasudevan. NeuTra-lizing bad geometry in hamiltonian monte carlo using neural transport. URL <http://arxiv.org/abs/1903.03704>.
- [14] J. D. Hunter. Matplotlib: A 2d graphics environment. 9(3):90–95. ISSN 1521-9615. doi: 10.1109/MCSE.2007.55. URL <http://ieeexplore.ieee.org/document/4160265/>.
- [15] G. Kanwar, M. S. Albergo, D. Boyda, K. Cranmer, D. C. Hackett, S. Racanière, D. J. Rezende, and P. E. Shanahan. Equivariant flow-based sampling for lattice gauge theory. 125(12):121601. ISSN 0031-9007, 1079-7114. doi: 10.1103/PhysRevLett.125.121601. URL <https://link.aps.org/doi/10.1103/PhysRevLett.125.121601>.
- [16] R. Kumar, C. Carroll, A. Hartikainen, and O. Martin. ArviZ a unified library for exploratory analysis of bayesian models in python. 4(33):1143. ISSN 2475-9066. doi: 10.21105/joss.01143. URL <http://joss.theoj.org/papers/10.21105/joss.01143>.
- [17] D. Levy, M. D. Hoffman, and J. Sohl-Dickstein. Generalizing hamiltonian monte carlo with neural networks. URL <http://arxiv.org/abs/1711.09268>.
- [18] Z. Li, Y. Chen, and F. T. Sommer. A neural network MCMC sampler that maximizes proposal entropy. URL <http://arxiv.org/abs/2010.03587>.
- [19] M. Medvidovic, J. Carrasquilla, L. E. Hayward, and B. Kulchytskyy. Generative models for sampling of lattice field theories. URL <http://arxiv.org/abs/2012.01442>.
- [20] Y. Nagai and A. Tomiya. Gauge covariant neural network for 4 dimensional non-abelian gauge theory. URL <http://arxiv.org/abs/2103.11965>.
- [21] K. Neklyudov and M. Welling. Orbital MCMC. URL <http://arxiv.org/abs/2010.08047>.
- [22] K. Neklyudov, M. Welling, E. Egorov, and D. Vetrov. Involutive MCMC: a unifying framework. URL <http://arxiv.org/abs/2006.16653>.
- [23] F. Perez and B. E. Granger. IPython: A system for interactive scientific computing. 9(3): 21–29. ISSN 1521-9615. doi: 10.1109/MCSE.2007.53. URL <http://ieeexplore.ieee.org/document/4160251/>.
- [24] D. J. Rezende, G. Papamakarios, S. Racanière, M. S. Albergo, G. Kanwar, P. E. Shanahan, and K. Cranmer. Normalizing flows on tori and spheres. URL <http://arxiv.org/abs/2002.02428>.
- [25] C. P. Robert. The metropolis-hastings algorithm. URL <http://arxiv.org/abs/1504.01896>.

- [26] S. Schaefer, R. Sommer, and F. Virotta. Investigating the critical slowing down of QCD simulations. In *Proceedings of The XXVII International Symposium on Lattice Field Theory — PoS(LAT2009)*, page 032. Sissa Medialab. doi: 10.22323/1.091.0032. URL <https://pos.sissa.it/091/032>.
- [27] A. Sergeev and M. Del Balso. Horovod: fast and easy distributed deep learning in TensorFlow. URL <http://arxiv.org/abs/1802.05799>.
- [28] A. Tanaka and A. Tomiya. Towards reduction of autocorrelation in HMC by machine learning. URL <http://arxiv.org/abs/1712.03893>.
- [29] M. Waskom, O. Botvinnik, D. O’Kane, P. Hobson, S. Lukauskas, D. C. Gemperline, T. Augspurger, Y. Halchenko, J. B. Cole, J. Warmenhoven, J. De Ruiter, C. Pye, S. Hoyer, J. Vanderplas, S. Villalba, G. Kunter, E. Quintero, P. Bachant, M. Martin, K. Meyer, A. Miles, Y. Ram, T. Yarkoni, M. L. Williams, C. Evans, C. Fitzgerald, Brian, C. Fonnesbeck, A. Lee, and A. Qalieh. mwaskom/seaborn: v0.8.1 (september 2017). URL <https://zenodo.org/record/883859>.
- [30] A. Wehenkel and G. Louppe. You say normalizing flows i see bayesian networks. URL <http://arxiv.org/abs/2006.00866>.

A. Appendix

A.1 Force Term

We can write the force term as

$$F = -\frac{1}{\lambda^2} \sum_k \lambda^k \text{Tr} \left[i \left(UA - A^\dagger U^\dagger \right) \lambda^k \right] \quad (40)$$

where A is the sum over staples

$$A = \sum_{\mu \neq \nu} U_\mu(x + \hat{\mu}) U_\mu^\dagger(x + \hat{\nu}) U_\nu^\dagger(x) \quad (41)$$

$$+ \sum_{\mu \neq \nu} U_{-\nu}(x + \hat{\mu}) U_\mu^\dagger(x - \hat{\nu}) U_{-\nu}^\dagger(x). \quad (42)$$

Since, $i(UA - A^\dagger U^\dagger) \in \mathfrak{su}(3)$, we can write it in terms of the generators λ^k as

$$\sum_k \lambda^k \text{Tr} \left[\lambda^k \sum_j c_j \lambda^j \right] = \sum_k \sum_j c_j \lambda^j \text{Tr} [\lambda^k \lambda^j] \quad (43)$$

$$= \frac{1}{2} \sum_k \sum_j c_j t^k \delta_{jk} \quad (44)$$

$$= \frac{1}{2} \sum_k c_k t^k \quad (45)$$

consequently, we can simplify the force term as

$$F[U] = -\frac{1}{2g^2} i \left(UA - A^\dagger U^\dagger \right). \quad (46)$$

A.2 Topological Charge Q

In lattice field theory, the topological charge Q is defined as the 4D integral over spacetime of the topological charge density q . In the continuum,

$$Q = \int d^4x q(x), \text{ where} \quad (47)$$

$$q(x) = \frac{1}{32\pi^2} \epsilon_{\mu\nu\rho\lambda} \text{Tr} \{F_{\mu\nu} F_{\rho\lambda}\} \quad (48)$$

On the lattice, we choose a discretization⁴ $q_L(x)$ such that $Q = a^4 \sum_x q_L(x)$. The most obvious discretization of q_L uses the 1×1 plaquette $P_{\mu\nu}(x)$, and can be written as

$$q_L^{\text{plaq}}(x) = \frac{1}{32\pi^2} \epsilon_{\mu\nu\rho\lambda} \text{Tr} \{P_{\mu\nu}(x) P_{\rho\lambda}(x)\} \quad (49)$$

this has the advantage of being computationally inexpensive, but leads to lattice artifacts of order $\mathcal{O}(a^2)$.

⁴We are free to choose a specific discretization as long as it gives the right continuum limit